6th China–Japan–Korea Joint Symposium on Optimization of Structural and Mechanical Systems
June 22-25, 2010, Kyoto, Japan

Shape Optimization of Clamping Members of Frame-Supported Membrane Structures under Stress constraints

Jun Fujiwara [1], Taku Nakajima [2], Makoto Ohsaki [3], and Fumiyoshi Takeda [1]

[1]Technical Research Center, Taiyo Kogyo Corporation, Hirakata 573-1132, Japan
{fj003177, tf001163}@mb.taiyokogyo.co.jp
[2]Dept. of Architecture and Architectural Engineering, Kyoto University, Kyoto 615-8540, Japan
rp2-nakajima@archi.kyoto-u.ac.jp
[3]Dept. of Architecture, Hiroshima University, Higashi-Hiroshima 739-8527, Japan
ohsaki@hiroshima-u.ac.jp

Abstract
A method is presented for shape optimization of clamping members under stress constraints. The cross-section of member is modeled and discretized by plane-strain two-dimensional finite elements. The cross-section has specified topology with fixed number of holes. The shapes of exterior boundary and holes are described by line segments and spline curves. The design variables are the locations of control points, and the objective function is the total structural volume that is to be minimized. Constraints are given for the von Mises equivalent stresses of each element, where the stresses due to bending of the members are added. In order to reduce the number of constraints, the maximum stress among all the elements is approximated by the *p*-norm. A general purpose finite element solver called ABAQUS is used for analysis, and a nonlinear programming library called SNOPT [4] is used for optimization. For this purpose, an interface program is developed using a script language called Python. It is shown in the numerical examples that the total volume is effectively decreased by using the proposed method. The validity of two-dimensional model is also investigated through analysis of the three-dimensional model.

Keywords: *Membrane structure, Clamping member, Shape optimization, Stress constraints*

1. Introduction

In the field of architectural engineering, PTFE-coated glass fiber fabric, which is simply called membrane material, is widely used for lightweight roofs of long-span structures such as domes, stadiums, and gymnasiums. Since membrane materials can transmit only in-plane tensile forces, a membrane roof is stabilized and shaped into three-dimensional curved surface by pre-tensioning. A membrane roof is generally connected to boundary steel frames with clamping members called fasteners, which are usually made of aluminum alloy manufactured by extrusion molding. Since such aluminum clamping members are mass-products, total production cost of a membrane roof can be significantly reduced by optimizing the cross-sectional shape and topology of those members.

It is known that the shape and topology of a continuum can be effectively optimized using the well-developed methods such as solid isotropic material with penalization (SIMP) approach, homogenization method, and level-set approach. However, most of the practical applications are concerned with global structural performances such as compliance and eigenvalues of vibration. Therefore, optimization under local stress constraints is still difficult for large complex continuum structures. The third author presented a method to find shapes of beam flanges for maximizing the plastic energy dissipation under cyclic deformation [1, 2] as a first attempt of optimizing performances of mass-produced structural parts in the field of civil and architectural engineering.

In this study, we present a method for shape optimization of clamping members under constraints on von Mises equivalent stress. The cross-section of center span of the member supported by two bolts is discretized by two-dimensional finite elements with plane strains. The cross-section has specified topology with a hole. The shapes of boundary and hole are represented by line segments and spline curves. The design variables are the locations of control points. The objective function is the total structural volume that is to be minimized. The stresses due to bending moment under distributed membrane tensile force are added for evaluating the equivalent stress. In order to reduce the number of constraints, the maximum stress among all the elements is approximated by the *p*-norm.

A general purpose finite element solver called ABAQUS [3] is used for analysis, and a nonlinear programming library called SNOPT is used for optimization. Two programs are connected by an interface developed using a script language called Python. From the results of numerical examples, it is shown that the total volume is effectively decreased by using the proposed method. The validity of two-dimensional model is also verified through analysis of the three-dimensional

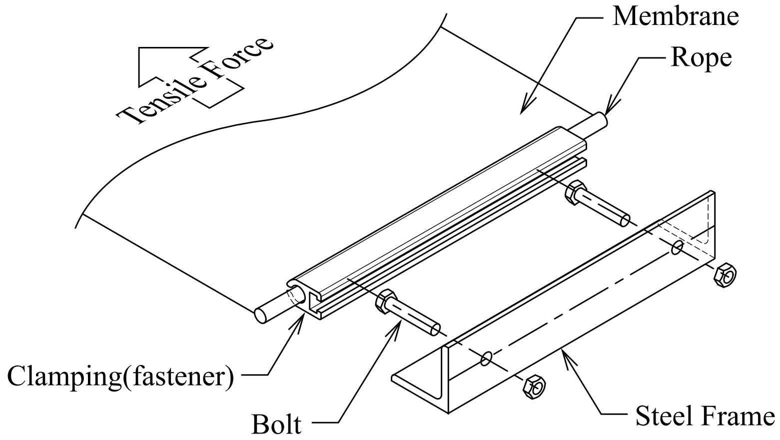

Figure 1. Clamping a membrane to a steel frame.

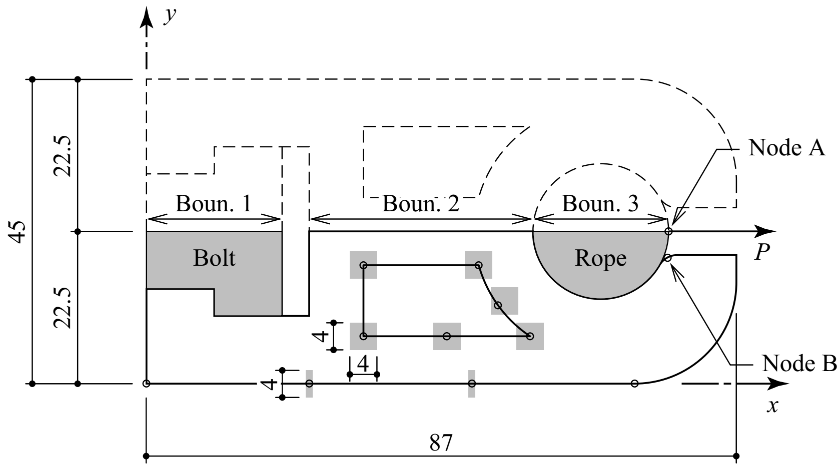

Figure 2. Section of clamping member.

model.

2. Optimization problem

Optimal shape is found for the clamping member as shown in Fig. 1. Since it is difficult to optimize the clamping using three-dimensional analysis, the clamping is first modeled as a two-dimensional finite element model and optimized, and three-dimensional analysis is carried out for additional modification of the sectional shape. The clamping member is subjected to the tensile force of membrane, and supported by two bolts at the ends of the clamping member. Therefore, based on symmetry of the structure, boundary condition, and loading condition, one of the half parts is optimized. Moreover, we first assume that the bolt is distributed throughout the clamping, and optimize the section supported by a bolt as shown in Fig. 2, where the boundary 1, and the boundaries 2 and 3 are supported by pin and horizontal (x-directional) roller, respectively. The tensile force of membrane is transmitted to the clamping through the contact between clamping and rope. We assume the frictionless contact between the rope and clamping.

The shapes of boundary and hole are defined using spline curves and line segments. Let $\boldsymbol{X}$ denote the vector of variable locations of the control points indicated by circles in Fig. 2. The variables are vertical coordinates of the two control points at the extenral boundary, and horizontal and vertical locations of the six control points at the boundary of hole; therefore, we have 14 variable components in $\boldsymbol{X}$. The upper and lower bounds for the components of $\boldsymbol{X}$ are given as ±2 mm of the initial locations in Fig. 2.

The tensile force of the membrane material is defined as the load P as shown in Fig. 2.

The optimal shape is found for minimizing the total structural volume $V(\boldsymbol{X})$ under stress constraints. Let $\bar{\sigma}$ denote the upper bound for the maximum value $\sigma^{\max}(\boldsymbol{X})$ of the von Mises equivalent stresses among those evaluated at all the

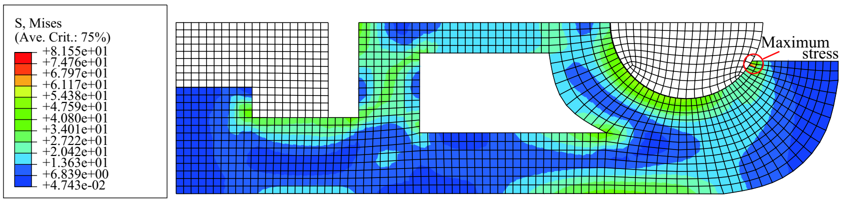

Figure 3. Stress distribution of initial shape utilizing contact.

integration points of all the elements. Then, the optimization problem for minimizing the total structural volume $V(\boldsymbol{X})$ is formulated as

$$\text{Minimize} \quad V(\boldsymbol{X}) \tag{1}$$

$$\text{subject to} \quad \sigma^{\max}(\boldsymbol{X}) \leq \bar{\sigma} \tag{2}$$

$$\boldsymbol{X}^{\mathrm{L}} \leq \boldsymbol{X} \leq \boldsymbol{X}^{\mathrm{U}} \tag{3}$$

where $\boldsymbol{X}^{\mathrm{U}}$ and $\boldsymbol{X}^{\mathrm{L}}$ are the upper and lower bounds for $\boldsymbol{X}$.

The quadrilateral plane-strain element CPE4R with reduced integration is used for discretization of the section of clamping, bolt and rope. The thickness of plate is 1 mm, and the FE-mesh is automatically generated with the nominal length 1 mm; hence, the numbers of elements and degrees of freedom are 2119 and 4648, respectively. Analysis is carried out using a finite-emenent analysis software called ABAQUS Ver 6.5.3 [3].

The material of the clamping member is an elastic aluminuum alloy categorized as AS-type. Type AS210 with nominal strength 210 N/mm^2, elastic moduls 7.0×10^4 N/mm^2, and Poisson's ratio 0.3 are used for optimization. The elastic moduli of the bolt and rope are ten times and 1/10 as large as that of the clamping.

The membrane is assumed to be a PTFE-coated glass fiber fablic called FGT-800. The thickness is 0.80 mm, nominal strength is 147.0 kN/m; hence, the distributed load applied to the rope is 73.5 kN/m, which is 1/2 of the nominal strength of the membrane.

A nonlinear programming software package SNOPT Ver. 7.2 [4] is used for optimization in conjunction with the analysis program package ABAQUS. The optimization algorithm is summarized as follows:

Step 1 Assign initial values for the design variables.

Step 2 Call a Python script from SNOPT to automatically generate FE-meshes and input file to ABAQUS, and execute ABAQUS for structural analysis.

Step 3 Extract the equivalent stresses at the integration points from the output file of ABAQUS using a Python script.

Step 4 Compute the values of objective and constraint functions.

Step 5 Update design variables in accordance with the optimization algorithm of SNOPT.

Step 6 Go to Step 2 if not converged.

3. Optimization results

We optimize the model shown in Fig. 2. The stress distribution of initial shape is shown in Fig. 3. The maximum equivalent stress is 81.55 N/mm^2, which is observed at the element near node B. The total vertical contact force is 55.16 N, and the horizontal and vertical displacements (mm) at node B are 0.049 and 0.052, respectively.

The stress distribution of optimal shape is shown in Fig. 4, where the location of maximum stress that is different from the initial solution is also indicated. The control points are located at the boundary of feasible regions. The values of the objective function V (mm^3) excluding rope and bolt at initial and optimal solutions are 1237.3 and 965.4, respectively, i.e., the structural volume is successfully reduced by optimization. The maximum stress (N/mm^2) at initial and optimal solutions are 81.55 and 117.0, respectively; therefore, the stress constraints are not active at initial and optimal solutions. The deformation scaled by 20 is as shown in Fig. 5. The horizontal and vertical displacements at the node B increased from 0.049 to 0.098 and 0.052 to 0.117, respectively, as the result of optimization. The vertical contact force decreases from 55.16 to 52.5.

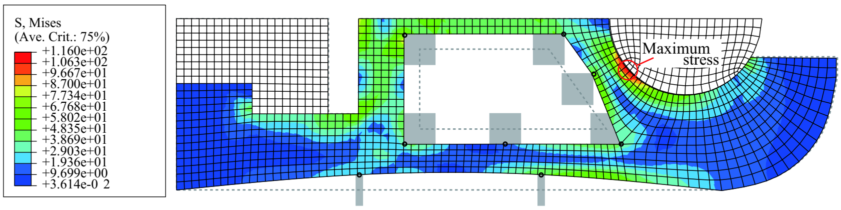

Figure 4. Optimal shape and its stress distribution.

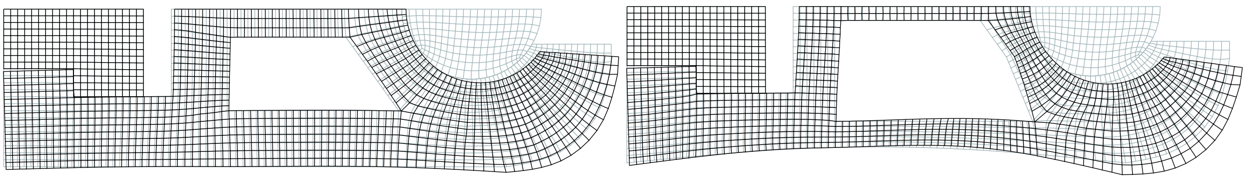

(a) (b)

Figure 5. Deformation scaled by 30; (a) initial, (b) optimal.

4. Optimization considering bending stress

In the previous example, the clamping member is supported by distributed bolts. However, in the parctical model, the clamping is supported by two anchor bolts, and the bending stress has the maximum value at the center of the clamping. Therefore, in this section, the bending stress σ^{b} due to the distributed load is added to the out-of-plane stress σ_{zz} of the plate model to optimize the section at the center of clamping member as

$$\sigma'_{zz} = \sigma_{zz} + \sigma^{\mathrm{b}} \tag{4}$$

Then the equivalent stress σ^{e} is computed as

$$\sigma^{\mathrm{e}} = \sqrt{\frac{1}{2}\{(\sigma_{xx} - \sigma_{yy})^2 + (\sigma_{yy} - \sigma'_{zz})^2 + (\sigma'_{zz} - \sigma_{xx})^2 + 6\sigma_{xy}^2\}} \tag{5}$$

In Step 3 of the algoritm in Sec. 2, the equivalent stresses at the integration points as well as their coordinates and covering areas are extracted from the output file of ABAQUS using a Python script. Then, the area and the second moment of intertia of the section can be easily computed to find the bending stress at each integration point.

In the previous section, a constraint was given for the maximum value of the stress evaluated at all the integration points. Since the point at which the stress takes the maximum value varies with the shape variation, the constraint is nonsmooth with respect to the design variables. In order to reduce nonsmoothness of the constraint, we approximate the maximum stress using the p-norm σ^{P} for the two largest stresses σ_{max1} and σ_{max2} as [5]

$$\sigma^{\mathrm{P}} = (\sigma_{\mathrm{max1}}^{p} + \sigma_{\mathrm{max2}}^{p})^{\frac{1}{p}} \tag{6}$$

with $p = 10$ in the following example. Fig. 6 shows the distribution of σ^{p} for $p = 5$ and 10, when σ_{max1} and σ_{max2} varies between 100 and 200.

The initial shape is as shown in Fig. 7, where the feasible regions of control points are also plotted. The radius of the right boundary is also added to the variable; therefore, the number of variables is 5. The distance between the bolts is 500 mm. The parameter p for the stress constraint is 10; therefore, $\sigma^{\mathrm{P}} = 1.071\sigma_{\mathrm{max1}}$ if $\sigma_{\mathrm{max1}} = \sigma_{\mathrm{max2}}$. At the initial solution, the maximum stress is $\sigma_{\mathrm{max}} = 170.0$ N/mm^2, and its value after smoothing is $\sigma^{\mathrm{P}} = 182.2$ N/mm^2, i.e., $\sigma^{\mathrm{P}}/\sigma_{\mathrm{max}} = 1.072$, which means that σ_{max1} and σ_{max2} are almost the same. The total structural volume is 911.6 mm^3, and the vertical contact force is 54.7.

The optimal shape is plotted in Fig. 8. The initial and optimal locations as well as the upper and lower bounds for the design variable are listed in Table 1. The total structural volume is 911.6 mm^3, horizontal and vertical diplacements at node B are 0.05 and 0.05, respectively, and the vertical contact force is 63.4. As is seen from Fig. 8, the width of the section is increased around the point of maximum stress, and is reduced in the region of small stress near the bolt, as a result of optimization. The width of circular part around the rope is also reduced.

The total structural volume decreased to 810.8 mm^3, which is about 66 % of 1237.3 mm^3 of the original shape. The horizontal and vertical displacements (mm) at node B are 0.17 and 0.21, respectively, which are sufficiently small. The

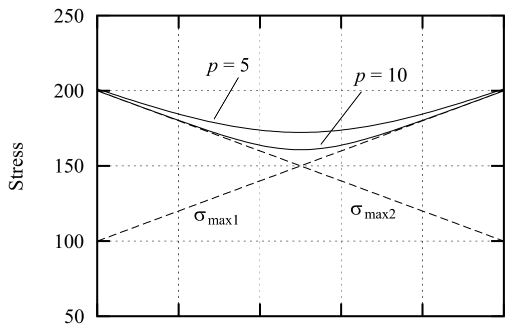

Figure 6. Smoothing using p-norm.

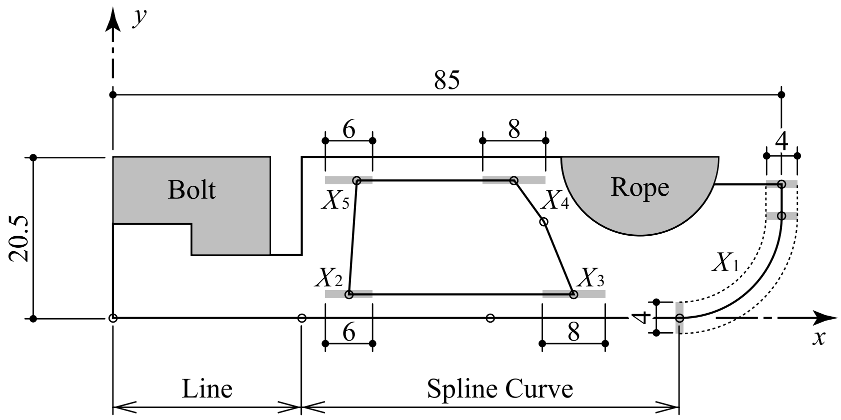

Figure 7. Initial shape.

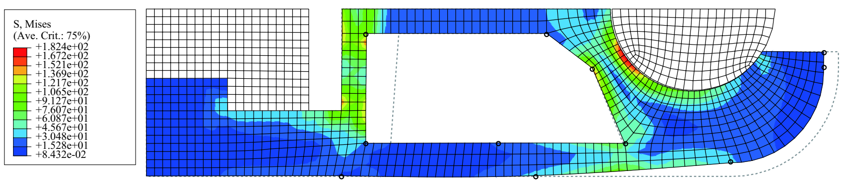

Figure 8. Optimal shape and its stress distribution.

maximum stress after smoothing is $\sigma^{\mathrm{P}} = 209.1\ \mathrm{N/mm^2}$, which is equal to the upper bound 210 $\mathrm{N/mm^2}$ with small tolerance. The actual maximum stress is 196.4 $\mathrm{N/mm^2}$.

5. Three-dimensional analysis.

Three-dimensional analysis is carried out for the initial and optimal solutions. The model consists of the clamping member, rope, and two bolts as shown in Figs. 9, 10, and Fig. 11, respectively. Some fillets are generated at the corners of the boundary of the clamping to prevent stress concentration. The type of bolt is M16, and the contact area between the clamping and bolt is 129.6 $\mathrm{mm^2}$ for each bolt. The material of bolt is steel with elastic modulus 2.05×10^5 $\mathrm{N/mm^2}$ and Poisson's ratio 0.3. Other material parameters are same as the two-dimensional model.

The eight node hexagonal solid element C3D8R with linear interpolation and reduced integration is used. Automatic mesh generation is used with the nominal size between 3 and 5 mm. The total structure without considering symmetry condition is analyzed. The distance between the bolts is 450 mm. The clamping, rope and bolts are assembled as shown in Fig. 12. The total numbers of elements and degrees of freedom are 23312 and 92952, respectively. All the translational and rotational displacements are fixed at the ends of the bolts. Only z-directional displacements are fixed at the two ends of the rope.

The stress distribution of the intial shape is shown in Fig. 13. The maximum stress of two-dimensional analysis

Table 1. Initial value X^0, optimal value X^{opt}, lower bound X^{L}, and upper bound X^{U} of the design variables.

	X^{L}	X^0	X^{U}	X^{opt}
X_1	11.00	13.00	15.00	11.24
X_2	27.00	30.00	33.00	27.00
X_3	54.57	58.57	62.57	58.87
X_4	46.00	50.00	54.00	49.16
X_5	27.00	31.00	33.00	27.00

is 137 N/mm^2 that is observed at the element in the left end of the clamping member. The stresses in section A are alsmost the same as those of two-dimensional analysis that includes the bending stress. As shown the section B in Fig. 13, however, large stress is observed at the contact point between the clamping and bolt. Large stresses are also seen in the bolts. Because bending deformation due to bending of the clamping is unreallystically constrained due to the fixed supports, the large stresses at the contact point are occured. Therefore, the rotation around the support should be allowed. The maximum stresses by two- and three-dimensional analyses are 137 N/mm^2 and 106 N/mm^2, respectively. The *x*-directional displacement at the section A by three-dimensional analysis is about 1 mm.

Three-dimensional analysis is also carried out for the optimal shape in Fig. 14. The stress distribution is as shown in Fig. 15. The *x*-directional displacements in section A are about 1.5 mm. Similarly to the three-dimensional analysis for the initial shape, the maximum stress at section B is seen at the contact point between clamping and bolt, and 358 N/mm^2. A stress about 300 N/mm^2 that exceeds the upper bound 210 N/mm^2 is also observed around the region S. The stress in this region is about 180N/mm^2 that is less than the upper bound.

We next investigate the applicability of plane strain element in the two-dimensional analysis. The stresses are compared in section B that does not have bending moment. Table 2 shows the stress and strain components of element E indicated in Fig. 15. As is seen, both of the out-of-plane stress and strain have nonzero values; therefore, the section exhibits an intermediate deformation between plane stress and plane strain.

If plane stress and plane strain elements are used in the two-dimensional analysis, the equivalent stress after adding bending stress are 250N/mm^2 and 196N/mm^2, respectively. Since the result by three-dimensional analysis is 186.3 N/mm^2, the plane strain element has better approximation.

Since it is difficult to optimize the clamping member using three-dimensional analysis, or accurately estimate the stresses in region S, the clamping is first optimized using two-dimensional model, and the shape around region S may be modified if necessary after three-dimensional analysis. The four points on the dotted line in Fig. 16 is moved to right

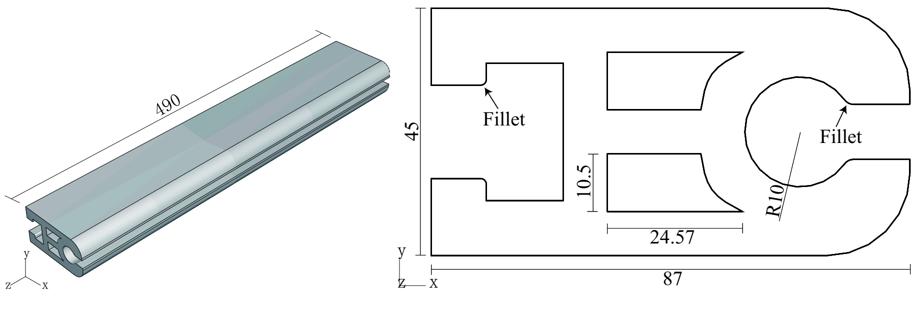

Figure 9. Dimension of clamping member.

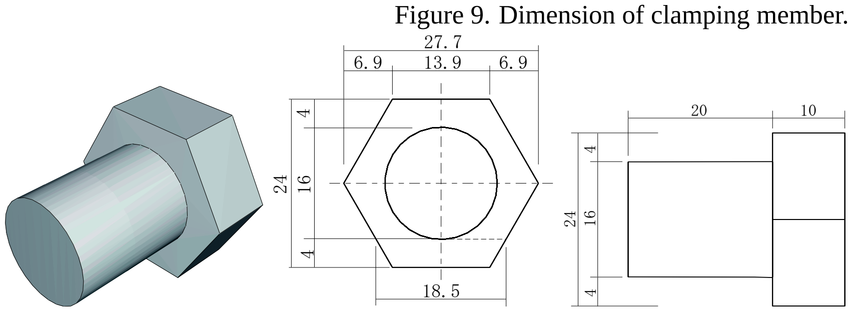

Figure 10. Dimension of anchor bolt.

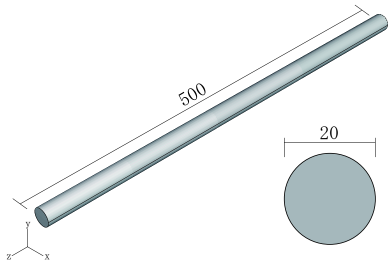

Figure 11. Dimension of rope.

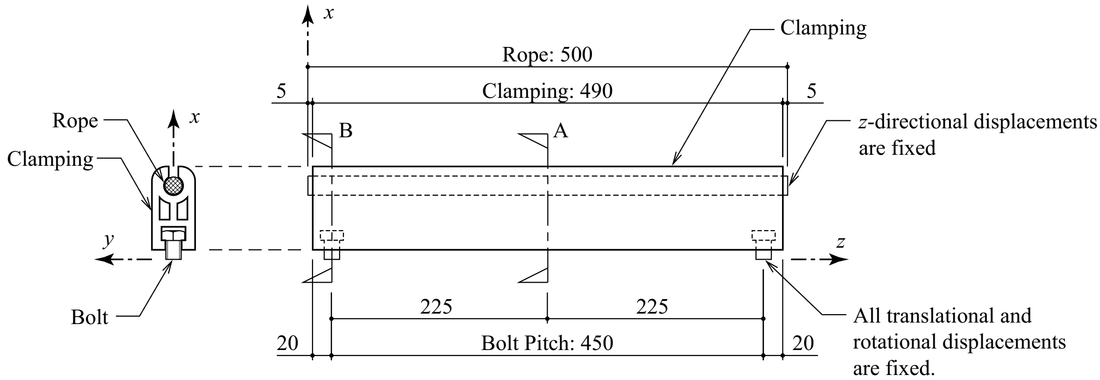

Figure 12. Assemblage of parts.

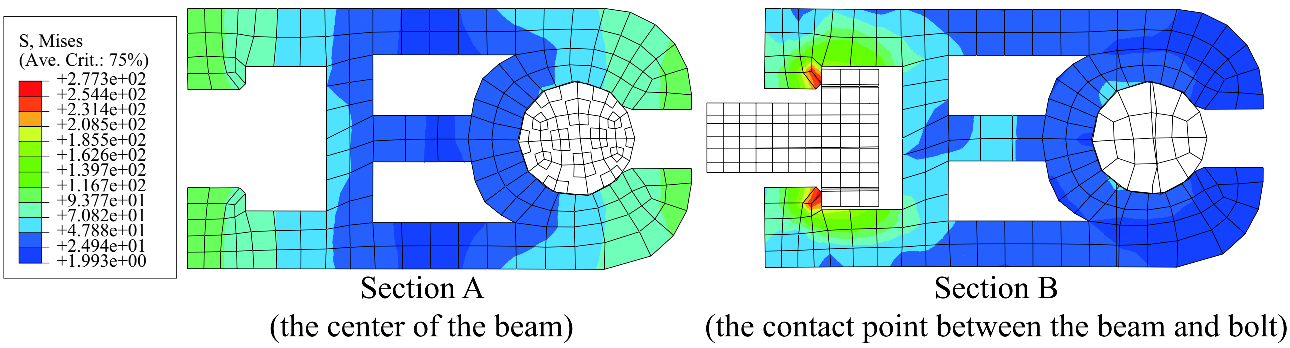

Figure 13. Stress distributions of section A,B ; three-dimensional models.

Table 2. Stress components σ_{ij} and strain components ε_{ij} of an element.

σ_{ij}	N/mm^2	ε_{ij}	($\times 10^{-3}$)
σ_{11}	0.6883	ε_{11}	-0.004775
σ_{12}	-1.6263	ε_{12}	-0.060346
σ_{13}	0.0670	ε_{13}	0.002135
σ_{22}	-0.3415	ε_{22}	-0.023689
σ_{23}	-4.5230	ε_{23}	-0.168055
σ_{33}	3.7269	ε_{33}	0.051742

consecutively by 1 mm, and the stresses are evaluated.

The stresses after modification of 3 mm is shown in Fig. 17. The maximum stresses around right and left ends of section A are 142.5 N/mm^2 and 142.1 N/mm^2, which are almost the same. The maximum stress excluding the contact point in section B is 192.7 N/mm^2, which is less than the upper bound. The total structural volume is increased by 81 mm^3 as the result of modification; however, ther reduction rate from the original shape is 30 %.

6. Conclusion

Shape optimization has been carried out for clamping members of membrane structures. The total structural volume is minimized under constraints on von Mises equivalent stress. It is shown that the total volume is effectively decreased by proposed method. The cross-section of the clamping member is discretized by two-dimensional finite elements with plane strains. The shapes of boundary and hole are represented by line segments and spline curves, and locations of some control points are considered as design variables.

The stresses due to bending moment under distributed membrane tensile force are added for evaluating the equivalent stress. The maximum stress among all the elements is approximated by the p-norm in order to reduce the number of constraints and nonsmoothness of the constraint function. It has been shown in the numerical examples that the structural

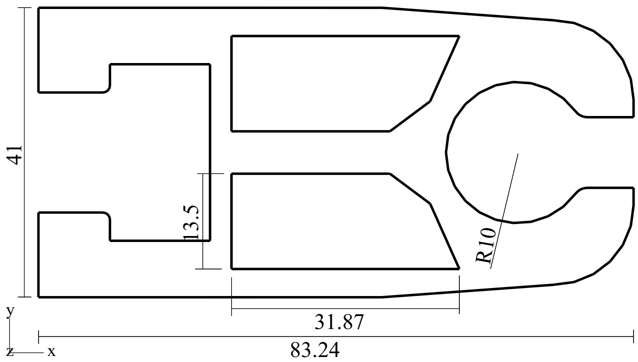

Figure 14. Dimension of optimal shape.

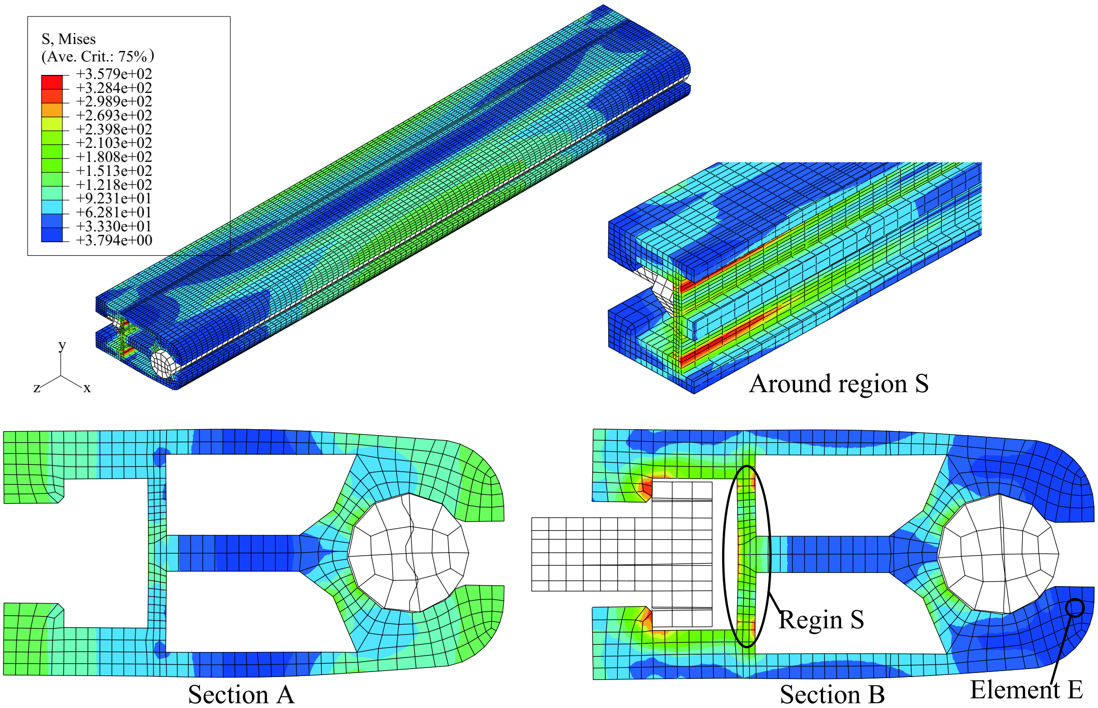

Figure 15. Stress distribution.

volume is successfully reduced by optimization.

Three-dimensional analysis is carried out for the initial and optimal solutions to verify applicability of two-dimensional model for optimization. The clamping member, two bolts, and the rope are discretized by three-dimensional solid elements. It has been shown that the section of the clamping member exhibits an intermediate deformation between plane stress and plane strain, and the plane strain element has better approximation of the three-dimensional analysis.

In the result of three dimensional analysis for the optimal shape, large stresses exceeding the admissible stress have been observed. We have modified the optimal shape based on the three dimensional analysis, and shown that the shape, which can satisfy the stress constrants and has sufficiently reduced structural volume, can be found by a small modification.

Acknowledgement
Financial support by Nohmura Foundation for Membrane Structure's Technology is gratefully acknowledged.

References

1. P. Pan, M. Ohsaki and H. Tagawa, Shape optimization of H-beam flange for maximum plastic energy dissipation, J. Struct. Eng., ASCE, Vol. 133(8), pp. 1176-1179, 2007.

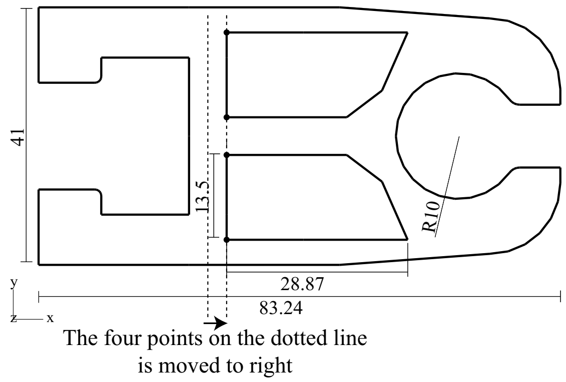

Figure 16. The model after modification.

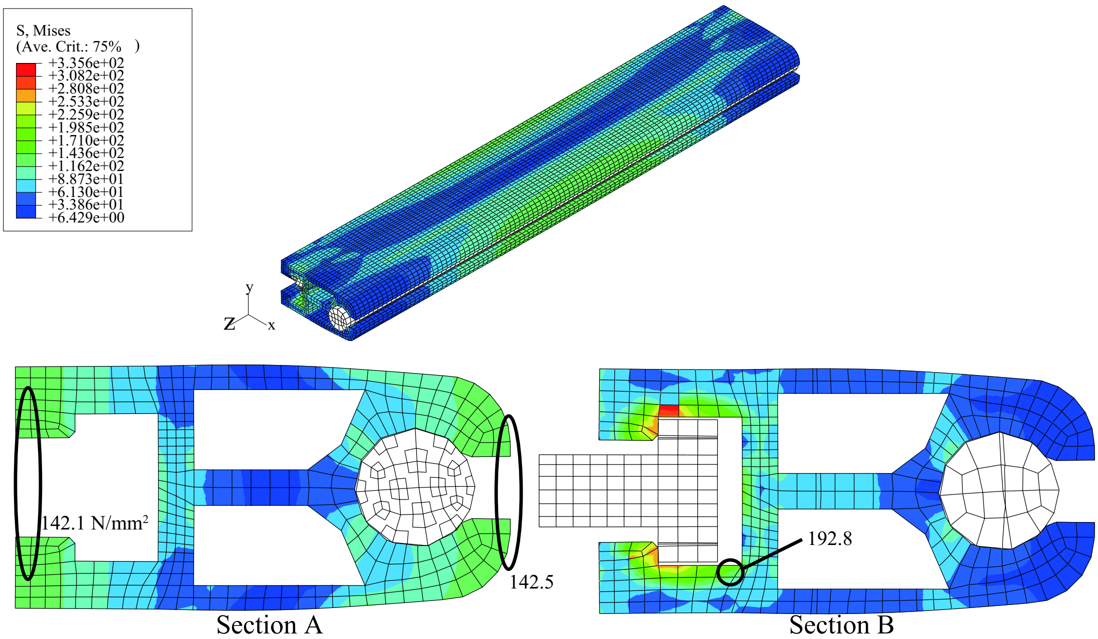

Figure 17. Stress distribution after modification.

2. M. Ohsaki, H. Tagawa and P. Pan, Shape optimization of reduced beam section for maximum plastic energy dissipation under cyclic loads, J. Constructional Steel Research, Vol. 65, pp.1511–1519, 2009.

3. ABAQUS Ver. 6.5.3 Documentation, ABAQUS Inc., 2006.

4. P. E. Gill, W. Murray and M. A. Saunders, SNOPT: An SQP algorithm for large-scale constrained optimization, SIAM J. Optim., Vol. 12, pp. 979–1006, 2002.

5. P. Duysinx and M. P. Bendsøe, Topology optimization of continuum structures with local stress constraints, Int. J. Numer. Methods Eng., Vol. 43, pp. 1453–1478, 1998.